



MINISTRY OF AVIATION
AERONAUTICAL RESEARCH COUNCIL

CURRENT PAPERS

Pitching Derivatives for a Gothic Wing Oscillating about a Mean Incidence

By

H.C. Garner, M.A., A.F.R.Ae.S.

and *Doris E. Lehrian*, B.Sc.

LONDON: HER MAJESTY'S STATIONERY OFFICE

1963

Price 3s 6d net

Pitching Derivatives for a Gothic Wing Oscillating
about a Mean Incidence

- by -

H. C. Garner, M.A., A.F.R.Ae.S.

and

Doris E. Lehrman, B.Sc.

February 1963

Summary

This note briefly introduces a non-linear theory of wings in slow pitching oscillation with leading-edge separation in incompressible flow. The oscillatory lift and pitching moment become linear functions of mean incidence. Comparisons with measured pitching derivatives are made for a gothic wing of aspect ratio 0.75.

Replaces NPL Aero Note No.1010-A.R.C.24,537.
Published with the permission of the Director, National
Physical Laboratory.

1. Introduction

It is known that leading-edge separation occurs on wings of low aspect ratio at incidence, particularly when the leading edge is sharp; in consequence, the steady aerodynamic forces are non-linear with incidence. There is a corresponding effect of mean incidence on oscillatory derivatives, as experimental data^{1,2} have already shown.

For pitching oscillations of small amplitude and frequency about zero mean incidence, measured values of the damping derivative at low speeds are usually in satisfactory agreement with values as calculated by linear lifting-surface theory³. This remains true for wings of low aspect ratio, as shown by Figs. 11 and 12 of Ref. 4 for delta ($A = 1$) and gothic ($A = 0.75$) planforms. Furthermore, the comparisons of the measured¹ and theoretical values for the gothic wing, reproduced in Fig. 1, show that slender-wing theory is inadequate.

In steady incompressible flow, the overall forces at high incidence can be estimated theoretically by using Gersten's⁵ mathematical model of the flow (Fig. 2) as the basis of a non-linear theory. In Ref. 6 this vortex model is used in conjunction with Multhopp's⁷ linear theory for steady flow, to give a numerical method for wings of arbitrary planform. Although the vortex model fails to provide the load distribution on swept wings with separated flow, the comparisons⁶ between calculated and measured lift and pitching moment indicate that in this respect the non-linear theory is a decisive improvement on linear theory for wings in steady flow. The non-linear effects grow as aspect ratio decreases and become important for the delta ($A = 1$) and gothic ($A = 0.75$) wings at fairly low incidences.

Clearly we need a theoretical method of calculating pitching derivatives, which allows for mean incidence. An extension of the lifting-surface method of Ref. 6 to low-frequency pitching oscillations is now in preparation⁸. This can also be regarded as an extension of the linear oscillatory theory of Ref. 3, compatible with Gersten's⁵ vortex model. The basic equation is set out in Section 2, while Section 3 summarizes the steps of the calculation in matrix notation.

In the final Section 4, comparisons of the oscillatory lift and pitching moment are made for the gothic wing tested by Bristol Aircraft Limited in Ref. 2. These experiments support the use of a theory in which effects of frequency and amplitude of oscillation are ignored, and they go some way towards justifying the assertion, that pitching derivatives should show a linear dependence on mean incidence.

2. Basic Theory

A non-linear lifting-surface theory for wings in slow pitching oscillation can be developed with the aid of Gersten's simplified model of steady incompressible separated flow (Fig. 2). The trailing vorticity is supposed to be convected from the wing in planar sheets inclined at half the instantaneous angle of incidence, i.e. $\frac{1}{2}[\alpha + \theta(t)]$, to the wing surface. It is possible to derive an expression for the upwash at the wing, in which α^3 , $\alpha^2\theta$, $\alpha\theta^2$, θ^2 and higher order terms are neglected, but α^2 and $\alpha\theta$ are included as well as the linear terms in α and θ . In fact the non-dimensional wing loading is written as

$$\frac{\Delta p}{\frac{1}{2}\rho U^2} = \ell = \ell_1\alpha + \ell_{11}\alpha^2 + \text{Re}\left[(\bar{\ell}_1\theta_0 + \bar{\ell}_{11}\alpha\theta_0)e^{i\omega t}\right], \dots (1)$$

where α is the mean incidence, $\theta = \text{Re}\left[\theta_0 e^{i\omega t}\right]$, $\bar{\ell}_1$ and ℓ_{11} are complex quantities.

Let the wing describe pitching oscillations of amplitude θ_0 and angular frequency ω about an axis $x = hc$, where \bar{c} is the geometric mean chord. Then the boundary conditions at the wing surface require that the upwash angle

$$\frac{w}{U} = -\alpha - \text{Re}\left[\left(1 + \frac{i\omega x}{U} - \frac{i\omega \bar{c}h}{U}\right)\theta_0 e^{i\omega t}\right] \dots (2)$$

over the planform S . In Ref. 8 it will be shown that the upwash angle is related to the wing loading in equation (1) by

$$\begin{aligned} \frac{w}{U} = & \frac{1}{8\pi} \iint_S (\ell_1\alpha + \ell_{11}\alpha^2) K(x - x', y - y') dx' dy' \\ & - \frac{\alpha}{8} \frac{\partial^2}{\partial y^2} \left(\int_{-\infty}^x \ell_1\alpha(x - x') dx' \right) \\ & + \text{Re} \left[\left\{ \frac{1}{8\pi} \iint_S (\bar{\ell}_1 + \bar{\ell}_{11}\alpha) K(x - x', y - y') dx' dy' \right. \right. \\ & - \frac{i\omega}{8\pi U} \iint_S (\bar{\ell}_1 + \bar{\ell}_{11}\alpha) \left(\int_{-\infty}^x K(x_0 - x', y - y') dx_0 \right) dx' dy' \\ & - \frac{\alpha}{8} \frac{\partial^2}{\partial y^2} \left(\int_{-\infty}^x \bar{\ell}_1(x - x') \left[1 - \frac{i\omega(x-x')}{U} \right] dx' \right) \\ & \left. \left. - \frac{\alpha}{8} \frac{\partial^2}{\partial y^2} \left(\int_{-\infty}^x \ell_1(x - x') dx' \right) \right\} \theta_0 e^{i\omega t} \right], \dots (3) \end{aligned}$$

where

$$K(x-x', y-y') = \frac{1}{(y-y')^2} \left\{ 1 + \frac{x-x'}{[(x-x')^2 + (y-y')^2]^{\frac{3}{2}}} \right\}.$$

It can be seen that equation (3) involves four distinct operators

$$\left. \begin{aligned} A\{\ell\} &= -\frac{1}{8\pi} \iint_S \ell(x', y') K(x-x', y-y') dx' dy' \\ B\{\ell\} &= -\frac{1}{8\pi c} \iint_S \ell(x', y') \left(\int_{-\infty}^x K(x_0-x', y-y') dx_0 \right) dx' dy' \\ C\{\ell\} &= -\frac{1}{8} \frac{\partial^2}{\partial y^2} \left(\int_{-\infty}^x \ell(x', y) (x-x') dx' \right) \\ D\{\ell\} &= -\frac{1}{8c} \frac{\partial^2}{\partial y^2} \left(\int_{-\infty}^x \ell(x', y) (x-x')^2 dx' \right) \end{aligned} \right\} \dots (4)$$

The first of these, $A\{\ell\}$, arises in steady linear lifting-surface theory and is fully discussed in Ref. 7. The operator $B\{\ell\}$, together with $A\{\ell\}$, forms the basis of Ref. 3. The third, $C\{\ell\}$, is derived from Gersten's model of steady separated flow and, together with $A\{\ell\}$, forms the basis of Ref. 6. The remaining operator, $D\{\ell\}$, is peculiar to the unsteady non-linear theory and will be discussed in Ref. 8.

3. Solution in Matrix Notation

In terms of the operators of equation (4), equations (2) and (3) combine to give

$$\begin{aligned}
 & A\{e_1\}\alpha + A\{e_{1,1}\}\alpha^2 - C\{e_1\}\alpha^2 \\
 & + \operatorname{Re} \left[\left(A\{\bar{e}_1\} + A\{\bar{e}_{1,1}\}\alpha - i\nu B\{\bar{e}_1\} - i\nu B\{\bar{e}_{1,1}\}\alpha \right. \right. \\
 & \left. \left. - C\{\bar{e}_1\}\alpha + i\nu D\{\bar{e}_1\}\alpha - C\{e_1\}\alpha \right) \theta_0 e^{i\omega t} \right] \\
 & = \alpha + \operatorname{Re} \left[(1 + i\nu\xi - i\nu h) \theta_0 e^{i\omega t} \right], \quad \dots (5)
 \end{aligned}$$

where $\xi = x/\bar{c}$ and the frequency parameter $\nu = \omega\bar{c}/U$. The steady and oscillatory parts of equation (5) become respectively

$$A\{e_1\} + A\{e_{1,1}\}\alpha - C\{e_1\}\alpha = 1 \quad \dots (6)$$

and

$$\begin{aligned}
 & A\{\bar{e}_1\} + A\{\bar{e}_{1,1}\}\alpha - C\{e_1 + \bar{e}_1\}\alpha \\
 & - i\nu(B\{\bar{e}_1\} + B\{\bar{e}_{1,1}\}\alpha - D\{\bar{e}_1\}\alpha) = 1 + i\nu(\xi - h). \quad \dots (7)
 \end{aligned}$$

In a collocation method, equations (6) and (7) are replaced by sets of equations and the operators (4) are treated as matrices. Then the right hand side of equation (6) becomes a column $\{\alpha_1\} = \{1\}$ representing unit values at specified collocation points. Similarly the right hand side of equation (7) becomes

$$(1 - i\nu h)\{\alpha_1\} + i\nu\{\alpha_2\},$$

where $\{\alpha_2\}$ denotes a column of values of $\xi = x/\bar{c}$ at the specified collocation points.

Equation (6) leads to the steady solution of Ref. 6,

$$\{e\} = \{e_1\}\alpha + \{e_{1,1}\}\alpha^2, \quad \dots (8)$$

where

$$\left. \begin{aligned}
 \{e_1\} &= A^{-1}\{\alpha_1\} \\
 \{e_{1,1}\} &= A^{-1}C\{e_1\}
 \end{aligned} \right\}.$$

Similarly the real parts of $\{\bar{e}_1\}$ and $\{\bar{e}_{1,1}\}$, determined by setting $\nu = 0$ in equation (7), are respectively $\{e_1\}$ and $2\{e_{1,1}\}$. Hence we may write

$$\left. \begin{aligned} \{\bar{e}_1\} &= \{e_1\} + iv\{e'_1\} \\ \{\bar{e}_{1,1}\} &= 2\{e_{1,1}\} + iv\{e'_{1,1}\} \end{aligned} \right\}, \quad \dots (9)$$

where the real quantities $\{e'_1\}$ and $\{e'_{1,1}\}$ remain to be chosen so that equation (7) is satisfied identically to first order in v . Thus

$$\begin{aligned} A\{e'_1\} + A\{e'_{1,1}\}\alpha - C\{e'_1\}\alpha \\ = B\{e_1\} + 2B\{e_{1,1}\}\alpha - D\{e_1\}\alpha - h\{\alpha_1\} + \{\alpha_2\}. \end{aligned} \quad \dots (10)$$

The terms independent of α in equation (10) lead to the linear solution of Ref. 3

$$\{e'_1\} = -h\{e_1\} + A^{-1}\{\alpha_2\} + A^{-1}B\{e_1\}. \quad \dots (11)$$

It then follows that

$$\{e'_{1,1}\} = A^{-1}C\{e'_1\} + 2A^{-1}B\{e_{1,1}\} - A^{-1}D\{e_1\}, \quad \dots (12)$$

where $\{e_1\}$, $\{e_{1,1}\}$ and $\{e'_1\}$ are given in equations (8) and (11).

The unsteady part of the non-dimensional wing loading in equation (1) is expressed as

$$\{e'\} = [\{e_1\} + 2\{e_{1,1}\}\alpha]\theta + [\{e'_1\} + \{e'_{1,1}\}\alpha]\frac{\bar{c}\dot{\theta}}{U}, \quad \dots (13)$$

where $\dot{\theta} = d\theta/dt$. The pitching derivatives are then derived from the lift and moment integrals

$$\left. \begin{aligned} z_{\theta}\theta + z_{\dot{\theta}}\frac{\bar{c}\dot{\theta}}{U} &= -\frac{1}{2}\iint_S \frac{e' dx' dy'}{S} \\ m_{\theta}\theta + m_{\dot{\theta}}\frac{\bar{c}\dot{\theta}}{U} &= \frac{1}{2}\iint_S \frac{e'(h\bar{c}-x') dx' dy'}{S\bar{c}} \end{aligned} \right\}. \quad \dots (14)$$

4. Comparisons with Experiment

Oscillatory experiments on several sharp-edged models of the same gothic planform ($A = 0.75$) are described in Refs. 1 and 2. The earlier measurements of Ref. 1 were made on two uncambered models of different maximum thicknesses ($0.082 c_r$ and $0.050 c_r$) by observing the decay of pitching oscillations about each of three axes $h = 0.499, 0.724, 0.949$; only the damping derivative was obtained. The later measurements of Ref. 2 on another uncambered model of the smaller maximum thickness $0.050 c_r$ were carried out by forced pitching oscillation about two axes $h = 0.499$ and 0.949 ; the results are presented as complete sets of pitching and heaving derivatives for the axis $h = 0.724$. The effects of amplitude and frequency parameter on the pitching derivatives are small and within experimental error, but significant effects of mean incidence are found. Relative to the leading apex the planform is defined as follows:

$$\left. \begin{array}{ll} \text{leading edge} & x = x_\ell = c_r \left[1 - \sqrt{1 - (y/s)} \right] \\ \text{trailing edge} & x = x_t = c_r \\ \text{semi-span} & s = \frac{1}{4} c_r \\ \text{mean chord} & \bar{c} = \frac{2}{3} c_r \end{array} \right\}, \dots (15)$$

where c_r denotes the root chord. Calculations for this planform have been made with 7 spanwise and 3 chordwise collocation stations, i.e. 12 collocation points on the half wing.

The results in Figs. 18 and 19 of Ref. 2 include static measurements of lift and pitching moment about the axis $x = h\bar{c} = 0.724\bar{c}$. The coefficients

$$\left. \begin{array}{l} C_L = \iint_S \frac{\Delta p}{\frac{1}{2}\rho U^2} \frac{dx' dy'}{S} \\ C_m = \iint_S \frac{\Delta p}{\frac{1}{2}\rho U^2} \frac{(h\bar{c} - x')}{\bar{c}} \frac{dx' dy'}{S} \end{array} \right\} \dots (16)$$

from experiment and from equation (8) are compared in Fig. 3. The two sets of experimental data correspond to some previous balance measurements (\square) about the axis $h = 0.724$ and a

mean (α) from the wind-tunnel balance measurements of Ref. 2 about the two axes $h = 0.499$ and $h = 0.949$. The graphs of C_L against α and C_m show how greatly the non-linear steady theory of Ref. 6 improves on the results of linear theory.

As we have already seen in Fig. 1, the linear pitching damping from the theory of Ref. 3 is in good agreement with the various experimental results from Refs. 1 and 2 for a zero mean incidence. Also shown in Fig. 1 is a less satisfactory curve from slender-wing theory, which gives

$$\left. \begin{aligned} -z_{\theta} &= \frac{1}{4}\pi A \\ -z_{\dot{\theta}} &= \frac{1}{4}\pi A(2.3 - h) \\ -m_{\theta} &= \frac{1}{4}\pi A(0.7 - h) \\ -m_{\dot{\theta}} &= \frac{1}{4}\pi A(1.5 - h)^2 \end{aligned} \right\} \dots (17)$$

It is important to realise how wide of the mark this attractively simple linear theory can be, even for an aspect ratio as low as $A = 0.75$.

Relating to the gothic planform, Figs. 12, 13, 20, 21, 40 to 42 of Ref. 1 show little consistent effect of frequency parameter over the available range $0 < \nu = \omega c/U < 0.7$, but there are indications of a systematic dependence of $-m_{\dot{\theta}}$ on α . The values of the pitching damping for $\alpha = 20^\circ$ are plotted against axis position in Fig. 4. The formula (13) corresponding to the non-linear theory of Ref. 8 represents a significant improvement on the linear theory of Ref. 3 for the experimental range of axis position. For the rearmost axis $h = 0.949$, however, the new theory is not entirely satisfactory. The nature of this deficiency becomes clearer when both lift and pitching-moment derivatives are considered.

Figs. 10 to 13 of Ref. 2 give the four derivatives for the pitching axis $h = 0.724$; the full curves against mean incidence adequately represent smoothed experimental values for any frequency parameter in the range $0 < \nu < 0.7$. The lift derivatives $-z_{\theta}$ and $-z_{\dot{\theta}}$ of equation (14) are presented in Fig. 5, the experimental points (\times) corresponding to the full curves in Figs. 10 and 12 of Ref. 2. For zero mean incidence the stiffness derivative $-z_{\theta}$ shows satisfactory agreement with equation (17) from slender-wing theory and with the non-linear lifting-surface theory which for $\alpha = 0$ reduces to Ref. 3; non-linear theory and experiment show fairly consistent large effects of α , and

values of $-z_{\dot{\theta}}$ at $\alpha = 15^\circ$ are more than double those at $\alpha = 0$. On the other hand, the cross damping derivative $-z_{\dot{\delta}}$ is less satisfactory. Only fair agreement is obtained between linear theory and experiment at $\alpha = 0$, and slender-wing theory gives a serious overestimate; moreover, linear theory, giving $-z_{\dot{\theta}} = 0.711$ for all α , seems preferable to the non-linear theory in this case. The direct derivatives $-m_{\dot{\theta}}$ and $-m_{\dot{\delta}}$ of equation (14) are presented similarly in Fig. 6. Both derivatives show fair agreement between theory and experiment at $\alpha = 0$, except that slender-wing theory greatly overestimates the pitching damping. Non-linear theory and experiment show identical effects of α on $-m_{\dot{\delta}}$. For both pitching-moment derivatives the non-linear theory offers a marked improvement on the linear theory of Ref. 3.

5. Concluding Remarks

Theoretical and experimental considerations point to large effects of mean incidence on oscillatory pitching derivatives for wings of moderate to low aspect ratio. For incompressible flow, a significant advance on linear lifting-surface theory has been made by means of Gersten's simplified model of separated flow, although it is recognised that this model is unrealistic and unreliable for the prediction of load distribution. The use of a theory for slow pitching oscillations is not too restrictive, since the experiments indicate that frequency effects are small. Although the calculated values of $-z_{\dot{\theta}}$ for the gothic wing leave scope for further improvement, the other three pitching derivatives show a fairly good agreement between experiment and non-linear theory. It is intended to examine the consequences of modifying the elementary vortex sheets of Gersten's model to represent rolled-up vortex elements.

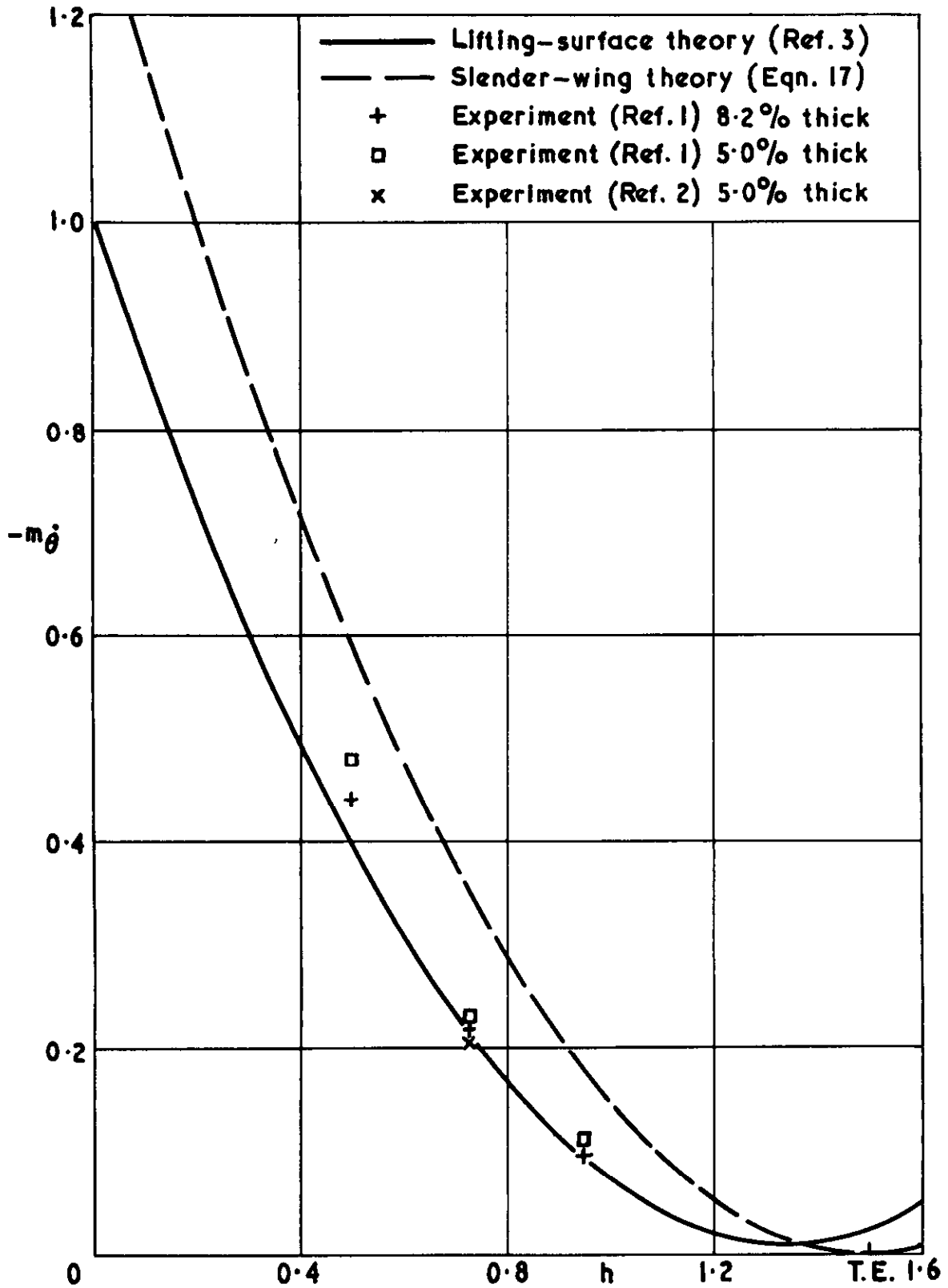
6. Acknowledgement

The authors acknowledge the assistance of Mrs. S. Lucas, who carried out the theoretical calculations and helped to prepare the diagrams.

References

<u>No.</u>	<u>Author(s)</u>	<u>Title, etc.</u>
1	J. G. Wright and Miss A. Wilkinson	Low speed wind-tunnel measurement of oscillatory derivatives for a family of slender wings. Part II, Damping in pitch. Bristol Aircraft Ltd. Report W.T.348. May, 1960.
2	J. G. Wright	Low speed wind tunnel measurements of the oscillatory longitudinal derivatives of a gothic wing of aspect ratio 0.75. MoA S & T Memo 1/62. A.R.C.24,357. April, 1962.
3	H. C. Garner	Multhopp's subsonic lifting-surface theory of wings in slow pitching oscillations. A.R.C. R. & M.2885. July, 1952.
4	W. E. A. Acum and H. C. Garner	The estimation of oscillatory wing and control derivatives. A.R.C. C.P.623. March, 1961.
5	K. Gersten	Nichtlineare Tragflächentheorie insbesondere für Tragflügel mit kleinem Seitenverhältnis. Ingen-Arch., Vol 30, pp.431-452, 1961.
6	H. C. Garner and Doris E. Lehrman	Non-linear theory of steady forces on wings with leading-edge flow separation. NPL Aero Report No.1059. A.R.C.24,523. February, 1963.
7	H. Multhopp	Methods for calculating the lift distribution of wings. (Subsonic lifting-surface theory). A.R.C. R. & M.2884. January, 1950.
8	H. C. Garner and Doris E. Lehrman	Non-linear theory of wings in slow pitching oscillation with leading-edge flow separation. Report in preparation.

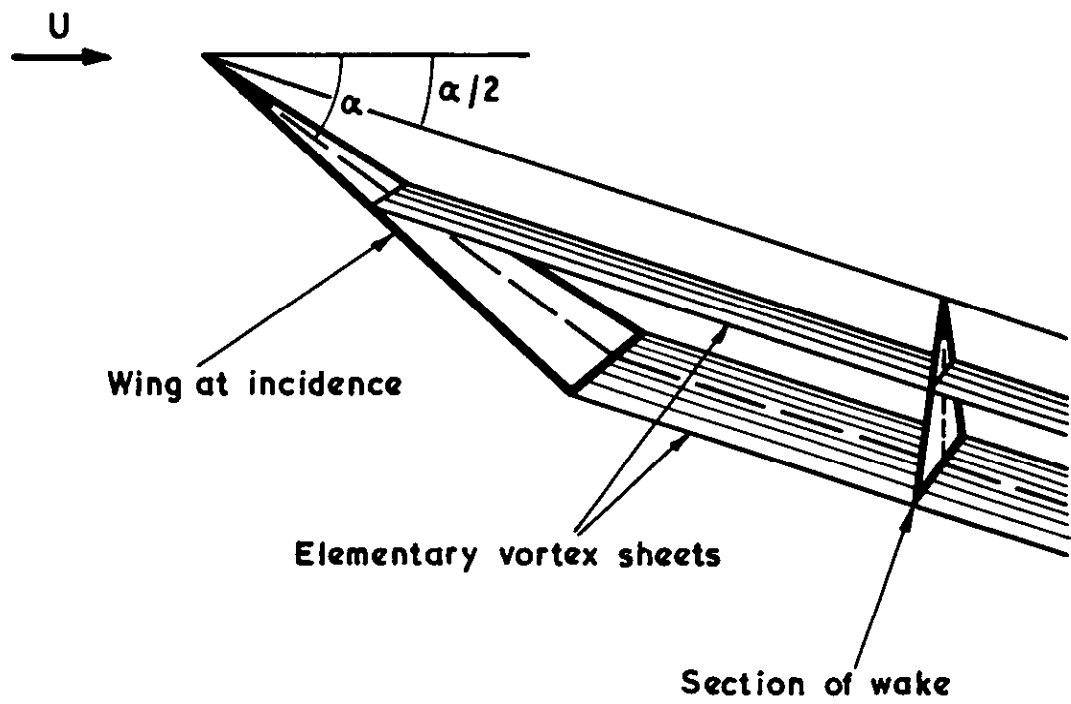
FIG. 1



Pitching damping against axis position for gothic wings

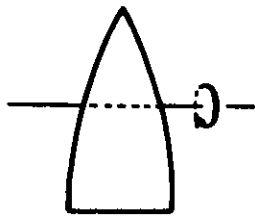
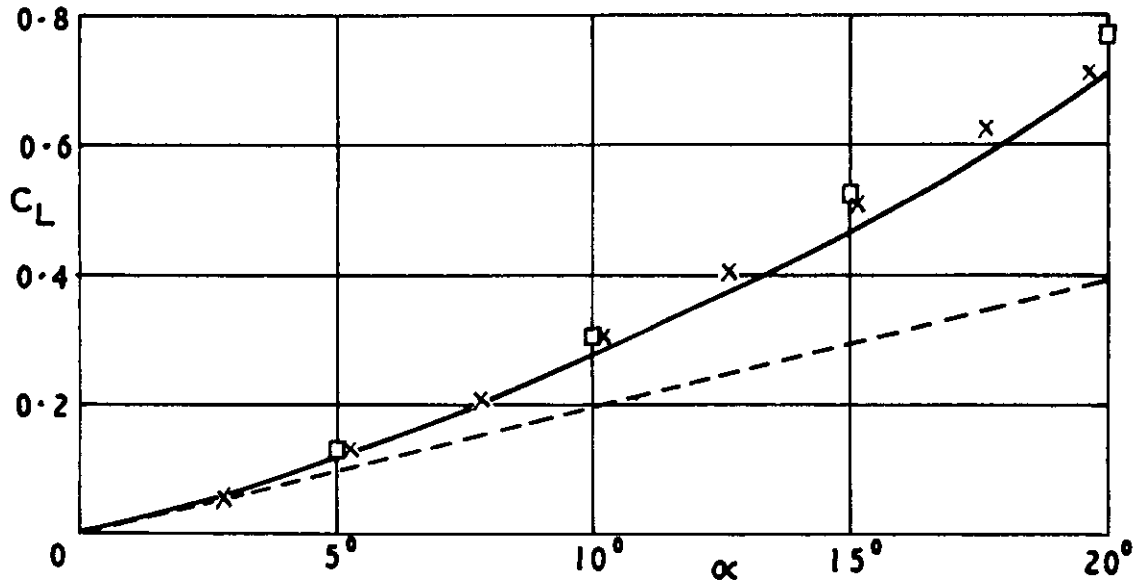
($A = 0.75$) at $\alpha = 0$

FIG. 2

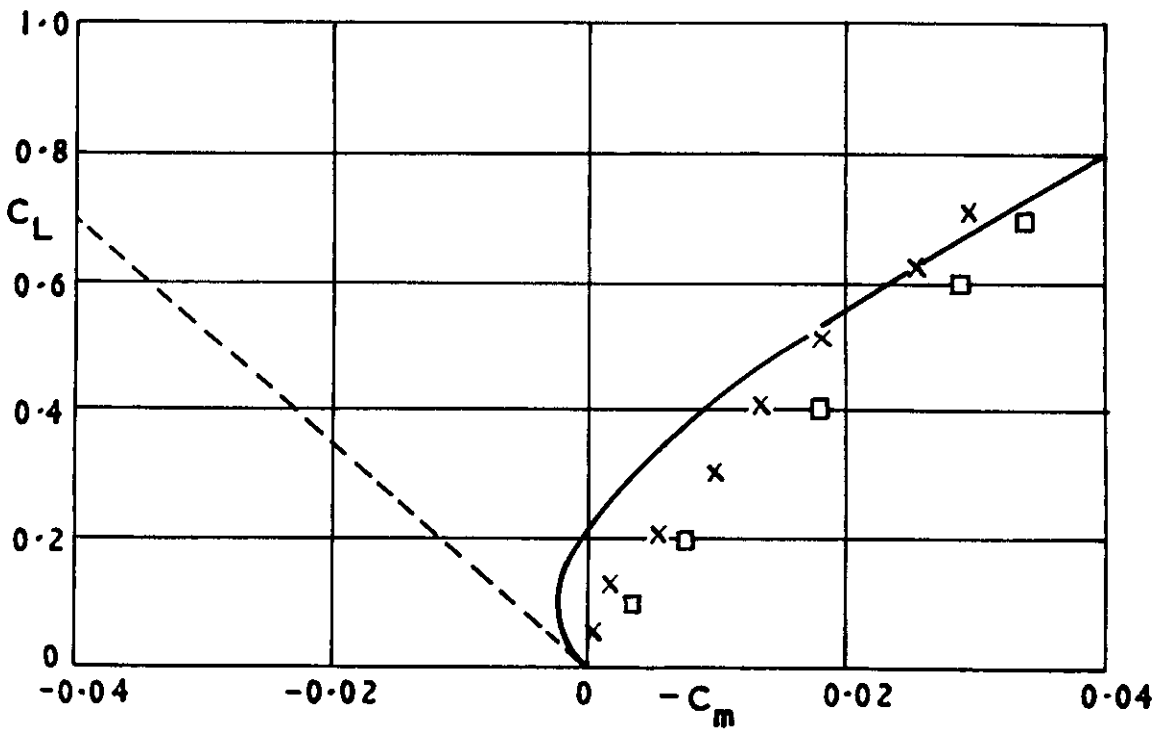


Vortex model of steady flow over a wing with
leading-edge separation

FIG. 3

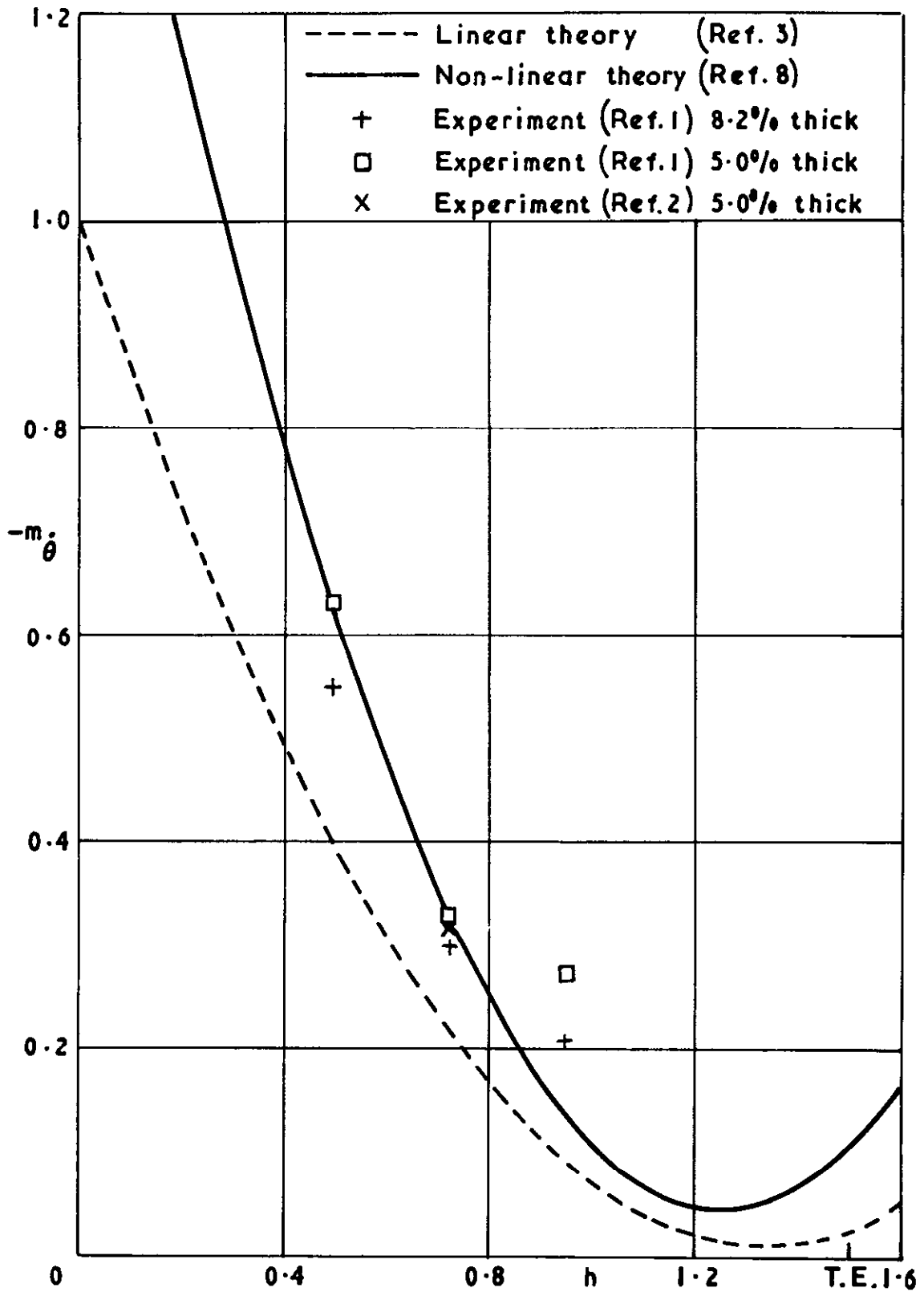


- Linear theory (Ref. 7)
- Non-linear theory (Ref. 6)
- Previous tests (Ref. 2)
- x W.T. balance (Ref. 2)



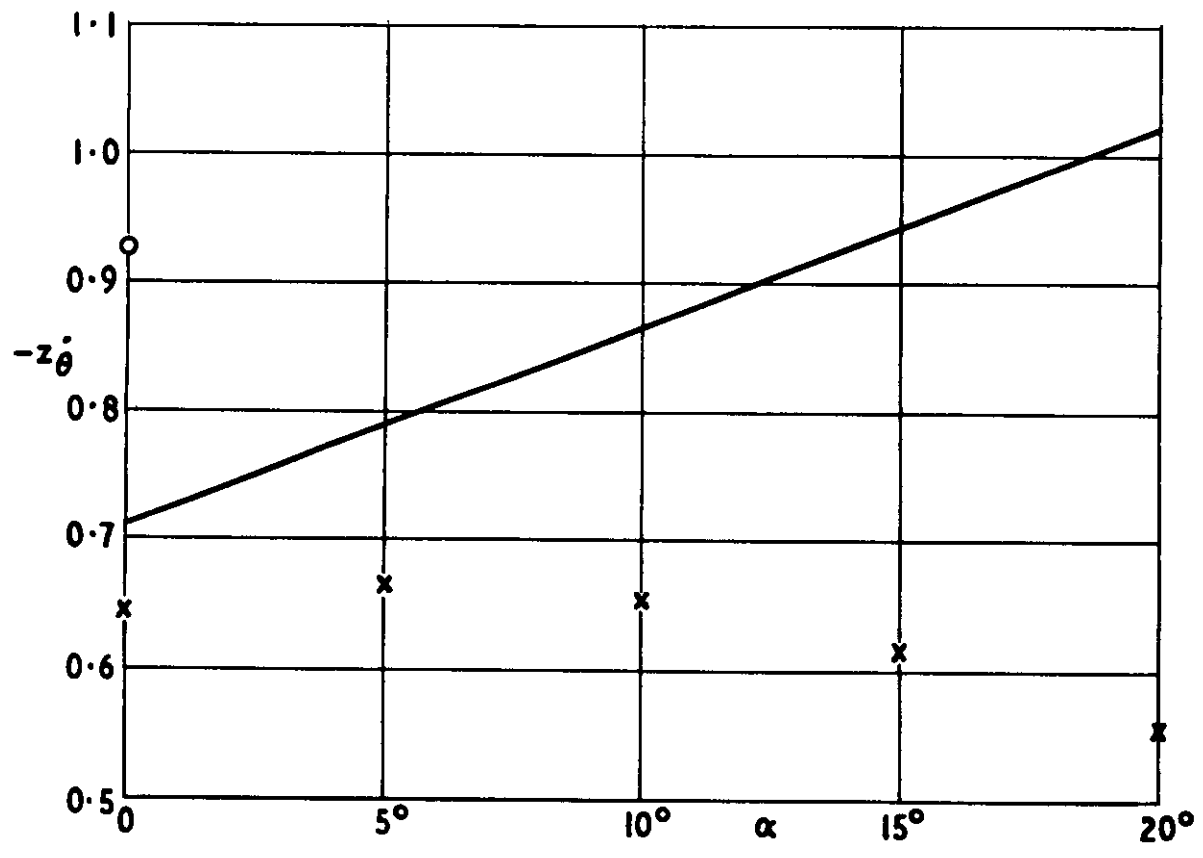
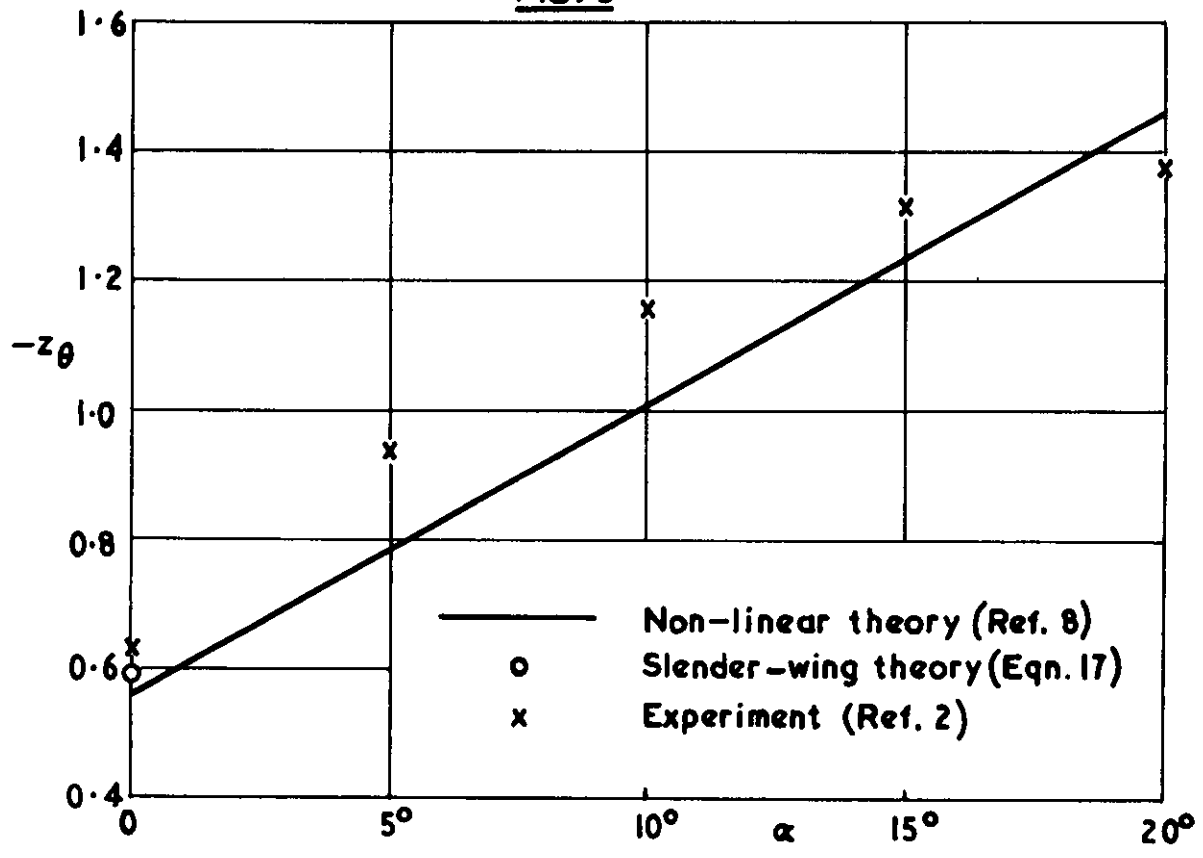
Steady lift against incidence and pitching moment ($h=0.724$)

FIG. 4



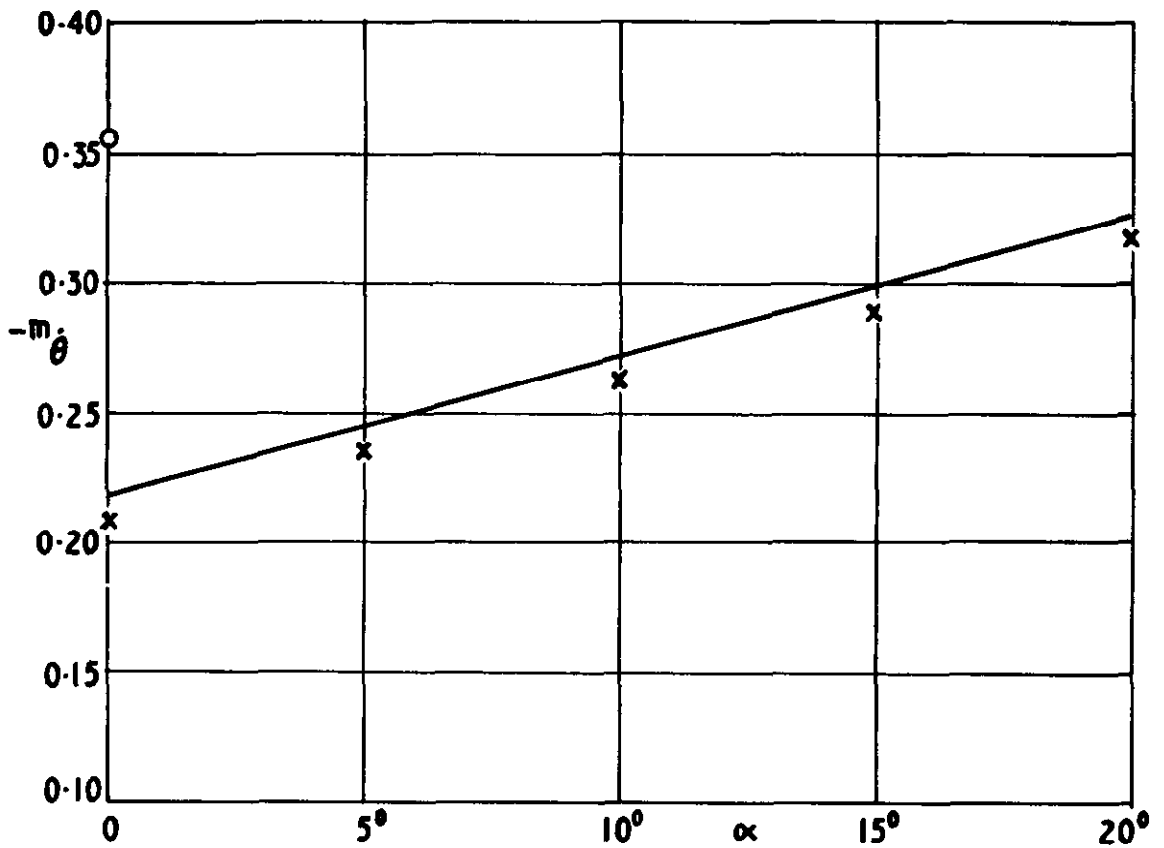
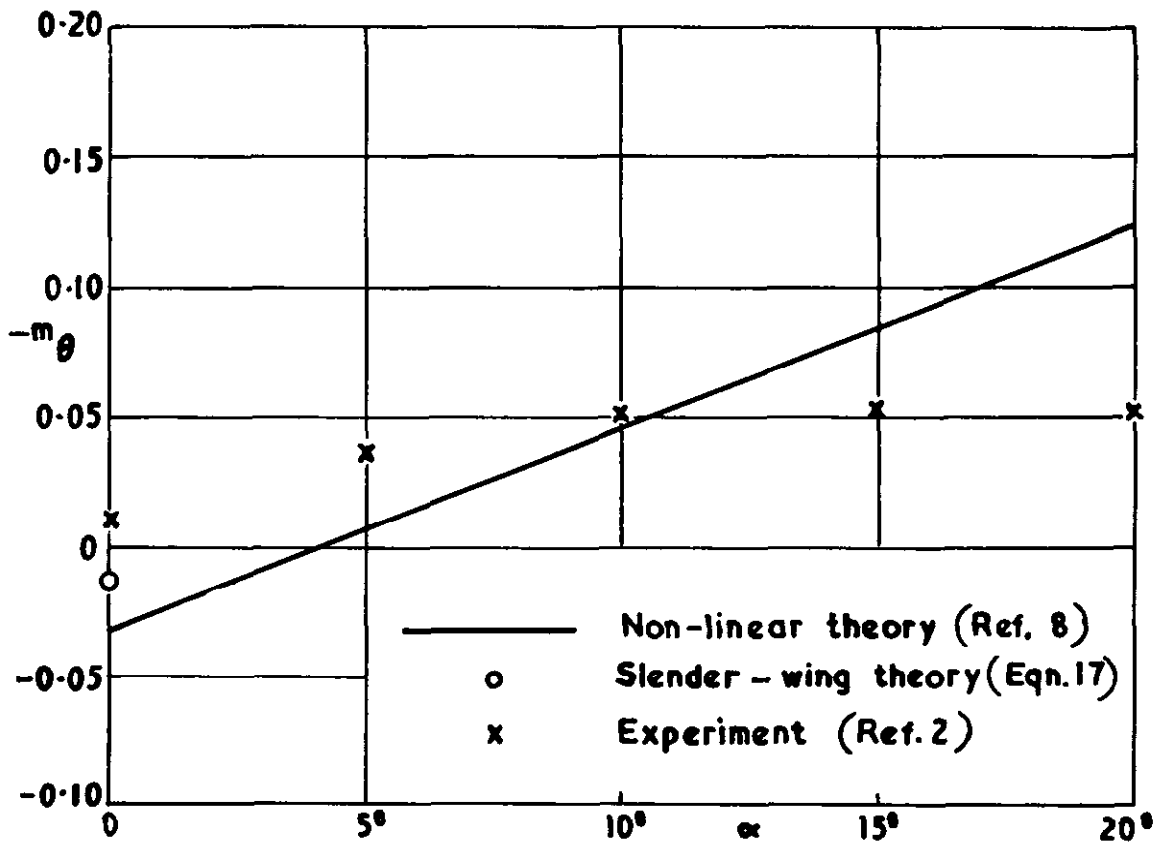
Pitching damping against axis position
for gothic wings ($A=0.75$) at $\alpha=20^\circ$

FIG. 5



Lift derivatives against mean incidence for pitching oscillations about $h = 0.724$

FIG. 6



**Direct pitching derivatives against mean incidence for oscillations
about $h = 0.724$**

A.R.C. C.P. No.695

February, 1963

Garner, H. C. and Lehrian, Miss D. E.

PITCHING DERIVATIVES FOR A GOTHIC WING
OSCILLATING ABOUT A MEAN INCIDENCE

This note briefly introduces a non-linear theory of wings in slow pitching oscillation with leading-edge separation in incompressible flow. The oscillatory lift and pitching moment become linear functions of mean incidence. Comparisons with measured pitching derivatives are made for a gothic wing of aspect ratio 0.75.

A.R.C. C.P. No.695

February, 1963

Garner, H. C. and Lehrian, Miss D. E.

PITCHING DERIVATIVES FOR A GOTHIC WING
OSCILLATING ABOUT A MEAN INCIDENCE

This note briefly introduces a non-linear theory of wings in slow pitching oscillation with leading-edge separation in incompressible flow. The oscillatory lift and pitching moment become linear functions of mean incidence. Comparisons with measured pitching derivatives are made for a gothic wing of aspect ratio 0.75.

A.R.C. C.P. No.695

February, 1963

Garner, H. C. and Lehrian, Miss D. E.

PITCHING DERIVATIVES FOR A GOTHIC WING
OSCILLATING ABOUT A MEAN INCIDENCE

This note briefly introduces a non-linear theory of wings in slow pitching oscillation with leading-edge separation in incompressible flow. The oscillatory lift and pitching moment become linear functions of mean incidence. Comparisons with measured pitching derivatives are made for a gothic wing of aspect ratio 0.75.



© *Crown copyright* 1963

Printed and published by
HER MAJESTY'S STATIONERY OFFICE

To be purchased from
York House, Kingsway, London w c 2
423 Oxford Street, London w 1
13A Castle Street, Edinburgh 2
109 St Mary Street, Cardiff
39 King Street, Manchester 2
50 Fairfax Street, Bristol 1
35 Smallbrook, Ringway, Birmingham 5
80 Chichester Street, Belfast 1
or through any bookseller

Printed in England